Hindawi
Shock and Vibration
Volume 2022, Article ID 2450513, 10 pages
https://doi.org/10.1155/2022/2450513

Research Article

Experimental Study of Prevention and Control of Rock Burst in Steeply Inclined Coal Seams by Mining Sequence and Filling

Zhihui Zhang, Yangyi Liu, Wenwen Zhu, Jian Liu, Tian Ma, and Chunxue Xie

School of Mechanics and Engineering, Liaoning Technical University, Fuxin 123000, China

Correspondence should be addressed to Zhihui Zhang; zhangzhihui@lntu.edu.cn

Received 1 September 2021; Revised 13 December 2021; Accepted 16 December 2021; Published 10 January 2022

Academic Editor: Jun Wang

The control and prevention of rock burst in a steeply inclined coal seam are essential. In order to figure out the effects of filling and mining sequence on rock burst in the steeply inclined coal seam, B3+6 and B1+2 coal seams in Wudong coal mine are chosen as the research objects, and an in-house experiment system of similarity simulation is established in this study. Combined with numerical simulation, the characteristics of collapse, stress distribution, and displacement variations can be measured, which provide useful information to study the effects of the filling body and mining sequence on rock burst. Experimental results show that the key reason for rock burst in a steeply inclined coal seam is the stress concentration of the rock pillar between B3+6 and B1+2 coal seams instead of the stress-lever-effect of a deeper rock pillar. The filling body can support the middle rock pillar, share the geological structure stress in the horizontal and vertical direction, eliminate the stress concentration zone largely, and prevent the occurrence of rock burst. When multiple working faces are working, the opposite side of the coal seam should be mined first to release the energy in the rock in advance, thus preventing the rock burst effectively. The research results provide fundamental information for better understanding the reason for rock burst and preventing rock burst in the steeply inclined coal seam.

1. Introduction

Recently, several rock bursts have occurred frequently during mining, especially in steeply inclined coal seams [1]. In addition, rock burst occurs at a depth that is shallower than the critical mining depth (500 m), making the mining of steeply inclined coal seams very difficult [2, 3]. According to statistics, steeply inclined coal seams account for above 50% of total mined seams in Western China [4, 5]. Xinjiang Autonomous Region is an important large-scale coal production base with hundreds of millions of tons of coal reserves, which account for more than 30% of global steep seam reserves [6]. Wudong coal mine, located in the east of Urumqi, is mined at a depth of less than 500 m, with the biggest dip angle of 83° and an average thickness of 40 m. Since September 2009, more than 10 rock bursts have occurred at B3+6 coal and B1+2 coal working faces at 300 m to 350 m depth [7]. The prevention and control of rock burst in steeply inclined coal seams have become an urgent problem.

Previous studies have revealed that the motion behavior of overburden strata in the steeply inclined working face is very different from that of flat seams [8], and the damage of rock pillars is the main reason for the rock burst in steeply inclined coal seams [9, 10]. The important role of the dip angle and the width of the coal pillar in the rock burst have been proposed, especially in inclined coal seams [11, 12]. To guide the prevention and control of rock burst, Lai et al. divided the roof failure period into three stages in which the accelerated active stage was the hazard preparation stage [13]. The numerical modeling method was used by Wang et al. to study the mechanisms and the prediction of rock bursts, which provides some references and guidelines for preventing and mitigating rock bursts in underground mines [14–16].

At present, the cut-and-fill mining technology is mostly applied to flat coal seams [17–19]. However, whether the cut-and-fill mining technology is effective to steeply inclined coal seams remains to be studied further. The physical similarity simulation test is a good way to solve the

complicated underground engineering problems compared with the calculation in theory only [20].

In this paper, a physical similarity simulation experiment based on B3+6 and B1+2 coal seams in the Wudong coal mine was designed to observe the stress and movement of overburden strata. Combined with the numerical simulation, the mining sequence and the filling body on the rock burst in steeply inclined extrathick coal seam were studied to prevent and control the rock burst in a similar steeply inclined coal seam.

2. Site Details of Wudong Coal Mine

The Wudong coal mine, with the surface at +800 m level, is located in the south of Dzungaria basin in Xinjiang Autonomous Region, China. The Wudong coal mine mainly exploits B3+6 and B1+2 coal seams with an average thickness of 40 m and 30 m separately and 83° dip angle. The B3+6 coal seam is a hard siltstone roof in the north of Wudong coal mine. The south of the Wudong coal mine has the B1+2 coal seam and the siltstone rock pillar with a width of 100 m. B3+6 and B1+2 coal seams are typical steeply inclined extrathick coal seams. The top-coal caving method has been used for mining. The height of the horizontal section is 25.0 m. The top-coal caving workings in the horizontal section are located beneath the multilayer mined-out area. The goaf is filled with yellow soil and has a space of 50 m under the surface (Figure 1).

3. The Similar Simulation Experiment

In this experiment, the influence of the mining sequence and the filling body on the movement, deformation, and stress change of overburden strata were studied by simulating the cut-and-fill mining process, from +800 m to +450 m levels of B3+6 and B1+2 coal seams.

3.1. Similar Condition. A similar simulation experiment should meet similarity condition: geometric similarity, density similarity, and stress similarity [21]. All the similarity conditions were designed according to the site mining conditions of B3+6 and B1+2 coal seams in the Wudong coal mine and laboratory conditions.

The geometric similarity constant:

$$C_l = \frac{L_P}{L_m}, \tag{1}$$

where L_p and L_m are the size of the prototype and the model, respectively. The mining depth of the Wudong coal mine is 440 m (L_p) from the surface to the +360 m mining level, and the height of the similar material simulation test bench is 2.2 m (L_m); therefore, $C_l = 200$.

The density similarity constant

$$C_d = \frac{D_p}{D_m}, \tag{2}$$

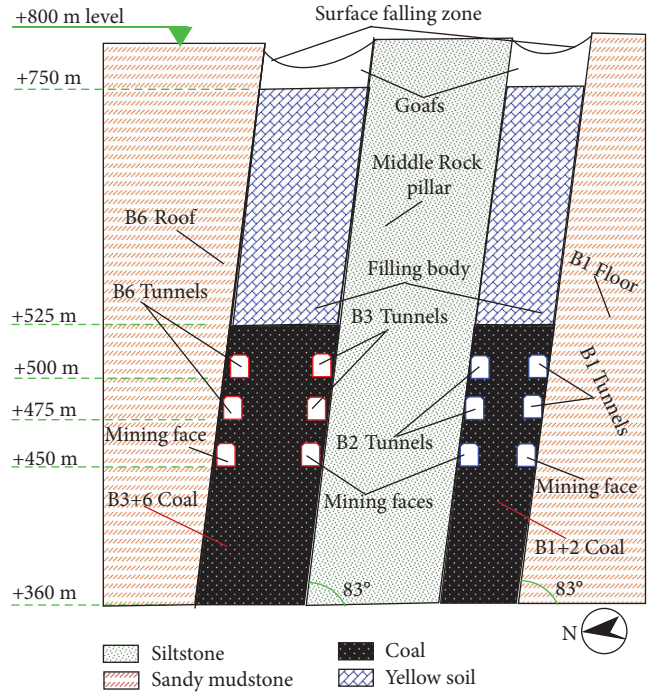

Figure 1: The profile of the Wudong coal mine.

where the density of the rock mass is 2.7 g/cm^3 (D_p), the density of similar material consolidation is 1.8 g/cm^3 (D_m), and $C_d = 1.5$.

The stress similarity constant

$$C_s = C_l \times C_d. \tag{3}$$

According to (1) and (2), $C_s = 300$.

3.2. Similar Materials. The choice of similar materials is very important. Similar materials should have the mechanical properties of the prototype as similar as possible and ensure the stability of the structure during the experiment. The rock destruction in the overburden strata is mostly caused by the tensile stress and compressive stress exceeding the uniaxial tensile and compressive strength of the rock, so the ratio of the compressive strength and tensile strength is taken as the main index in the experiment. The sand is used as an aggregate, and lime, cast, and water were used as cemented materials in this test [22]. All parameters are measured in the site and at lab (Table 1).

3.3. Instrument and Monitoring Points Layout. Experimental instruments comprise three parts, including a similar simulation system, movement observation system, and stress-monitoring and acquisition system.

3.3.1. Similar Simulation System. In this test, a multifunction microcomputer controlled electrohydraulic servo similar material simulation test system (DGS-8 type) was used to control the load. The test platform comprises a rigid loading frame, a similar materials filling tank, and 6 servo oil

Table 1: The parameter of the prototype and similar materials.

Rock property	Strength of the prototype (MPa)		Strength of the model (kPa)		σ_c/σ_t	L_p (m)	L_m (cm)	S/C	Proportion of materials		
	σ_c	σ_t	σ_c	σ_t					Lime	Cast	Water
Sandy mudstone	51.8	5.8	176.5	9.78	1 : 9	230	115	1 : 6	0.7	0.3	1 : 9
Siltstone	67.6	4.5	229.3	15.3	1 : 15	100	50	1 : 8	0.5	0.5	1 : 9
B3+6 coal	15.6	1.4	48.1	4.4	1 : 11	40	20	1 : 4	0.3	0.7	1 : 9
B1+2 coal	17.2	1.4	57.4	4.8	1 : 12	30	15	1 : 4	0.7	0.3	1 : 9

cylinders (4 upright oil cylinders and 2 horizontal oil cylinders), which can curb materials in a closed force space. The horizontal and vertical pressure produced from oil cylinders is controlled by using a computer strictly.

3.3.2. Movement Observation System. Xi'an Jiaotong University Digital Photogrammetry (XJTUDP), based on digital close-range industrial photogrammetry, is a portable optical 3D coordinate system to measure the coordinate of marks on the rock surface. In order to observe the displacement of overburdened strata, black grids (10×10 cm) are put on the surface in parallel and tangential ways to the seams. The intersections of the grids are marked as monitoring 418 points.

3.3.3. Stress Observation and Acquisition System. During the pouring, 24 pressure cells (BW-5 type) were arranged in the mold from +450 m level to +609 m level, in advance (Figure 2). The intelligent digital strain gauge (YJZ-32A type), linked to pressure cells, was used for logging real-time stress values. All data were analyzed by using the computer, and the laws of the stress in strata were concluded.

3.4. Facture of Model. There are four steeps: support, mixing, pouring, and demoulding.

(1) The support of almost vertical coal is different from that of the flat coal. Firstly, two templates were fixed on the front and back sides, and another template with a dip angle of 83° was fixed on the right side, according to the predesigned plan. Then, the monitoring points were put in the correct location as designed.

(2) According to Table 1, the amount (W) of each material needs to be calculated:

$$W = V \times D_m, \tag{4}$$

where V is the volume of each part, and D_m has the same meaning as (2).

The materials of each layer were put into a blender and mixed totally after the materials were weighted well.

(3) The materials in the blender were cleaned out and laid in strict accordance with the designed thickness, layer by layer. Mica powder was evenly sprinkled on every layer after compaction.

(4) The model was placed for 5–7 days. The templates were removed when the model was hard (Figure 3).

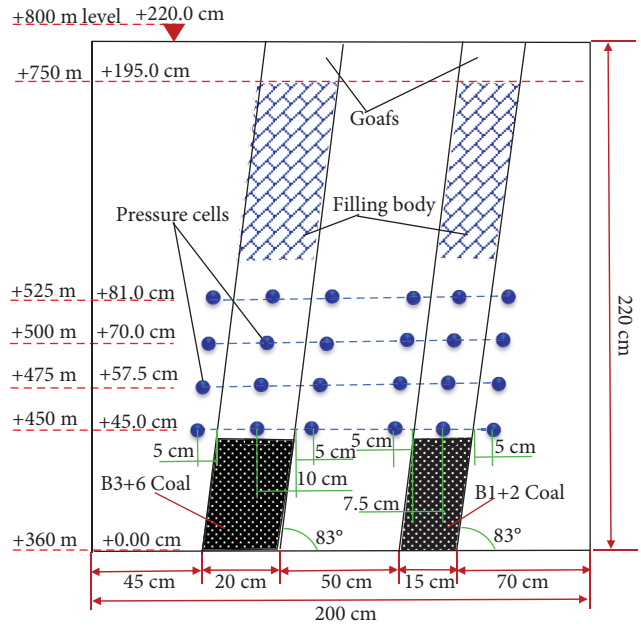

Figure 2: The layout of monitoring points.

3.5. Simulation of the Mining Process. According to the relatively complex geological conditions and mining process of the Wudong coal mine, the B3+6 and B1+2 goafs were filled with yellow soil, and the gangues had a space of 50 m under the surface after the +590 m level mining became stable. The loose yellow soil was put in a plastic bag as the filling body for simulation. In this small space, the loose yellow soil could deform under the pressure of rock pillars on both sides and support the surrounding rock with a certain strength. In order to highlight the mining sequence, the mining sequences have been changed three times successively (Table 2).

σ_c and σ_t are the compressive and tensile strength of the prototype and model material, respectively; L_p and L_m are the horizontal length of the prototype and model, respectively; and S/C is the ratio of the sand and cemented materials.

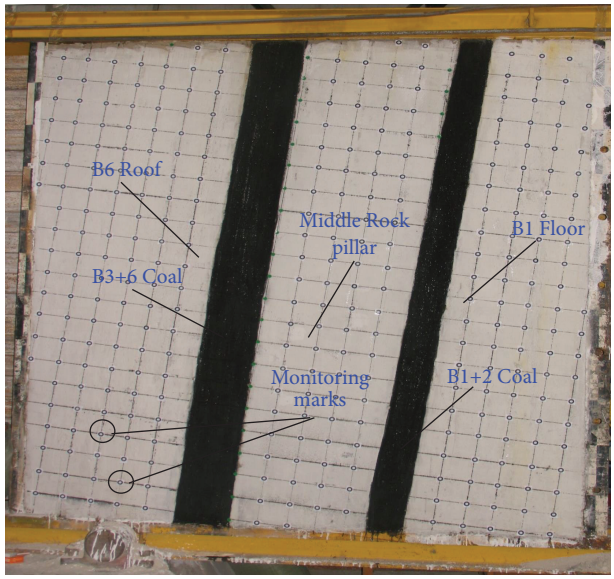

Figure 3: The physical model of similar simulation.

Table 2: The mining process.

Level	Mining sequence		Filling body	
	B3+6 coal	B1+2 coal	B3+6 goaf	B1+2 goaf
+525 m	1st	2nd	Filled	Filled
+500 m	2nd	1st	Filled	Removed
+475 m	1st	2nd	Filled	Removed
+450 m	2nd	1st	Filled	Removed

4. Numerical Simulation

According to the geological conditions of B3+6 coal and B1+2 coal in the Wudong coal mine, a two-dimensional computation model with a length of 400 m and a height of 440 m was established. After meshing the established model, a total of 33,860 entity type units were obtained, which satisfied the precision requirements of simulation calculation (Figure 4).

The mechanical parameters of the coal and rock all come from mechanics experiments and reference [23], as shown in Table 3. The Mohr–Coulomb constitutive model [24] was adopted in this numerical simulation. In order to reduce the stress concentration caused by constraints, the goaf was filled with the yellow soil to the surface, and the 50 m goaf was ignored in simulation. Because the yellow soil was loose, there was much space in the filling process; so, the internal friction angle of the yellow soil was reduced to 50%, and the tensile strength was 0. In the excavation, the softening modulus method was adopted to attenuate the elastic modulus of coal mass by 40%, releasing the stress.

5. Results and Discussions

In the mining of steeply inclined working face, the stability of overburden strata is affected by the fracture movement of roof-floor strata, the horizontal stress, and the gravity. When the tension or pressure exceed the tensile and pressure strength of the materials, the rock strata will be destroyed. The effect of filling and mining sequence on control and prevention of rock burst is studied by exploring the characteristics of fracture, displacement distribution law, stress distribution, and numerical simulation results.

5.1. The Characteristic of Fracture. Figures 5(a) and 5(b) show that when B1+2 coal seam are mined at +522 m level and +500 m level, the overburdened strata have not undergone significant deformation and collapse, and the overall structure is stable. Only one crack extends from the surface to the B6 roof rock strata. Due to the support of the yellow soil, the B6 roof and middle rock pillar do not have enough room to collapse.

When the B1+2 coal seam are mined at +500 m level, the yellow soil is removed artificially. After nearly 14 hours of evolution, rock mass fractures within 20 m range of the B2 roof developed further and finally fell towards the B1+2 gob. Without the yellow soil, the right side of the middle rock pillar in an independent state completely collapses. With the advance of the coal mining face, the cracks located at the middle rock pillar gradually develop from the top to the center, and the cracks in faults are accompanied by obvious changes.

Figure 4 shows that the middle rock pillar is damaged in the B2 roof but not in the rock pillars on the right side of the B3 laneway. The overall structure is stable, indicating that the reason for rock burst is not the stress-lever-effect of the deeper rock pillar but the high abnormal stress in the rock pillar in an independent state. This result is similar to the study conducted by Du et al. in 2018 [25].

5.2. Analysis of the Movement of Overburden Strata. In order to facilitate the analysis, the vectograph (Figure 6) was obtained from the XJTUDP system. According to the vectograph, the movement of every monitoring mark can be observed intuitionally. A longer arrow means that the value is greater.

Figure 6(a) shows that the values of the movement of the B6 roof are higher than those of other zones, and the maximum value is 15.68 mm. The movement of the rock pillar and B1 floor are less than 1.744 mm. Due to the horizontal and vertical geologic structural stress, the overburden strata generate displacement but no collapse with the filling yellow soil.

Figure 6(b) shows that when the filling body was removed, the values of the movement of the B2 roof at the middle rock pillar increase steeply, and the maximum value is 48.98 mm. The middle rock pillar collapsed, releasing energy, without the filling yellow soil, and also the displacement of the B6 roof increases slowly. However, the rock pillars on the right side of the B3 laneway do not generate any damage, and the displacement do not increase.

With the advancement of the coal mining face, the gob area and the transverse stress of overburdened strata expand. Therefore, the value of the movement of the B6 roof increases constantly. The value of the movement at the bottom of the B1 floor rises slowly, with a maximum value 8.514 mm.

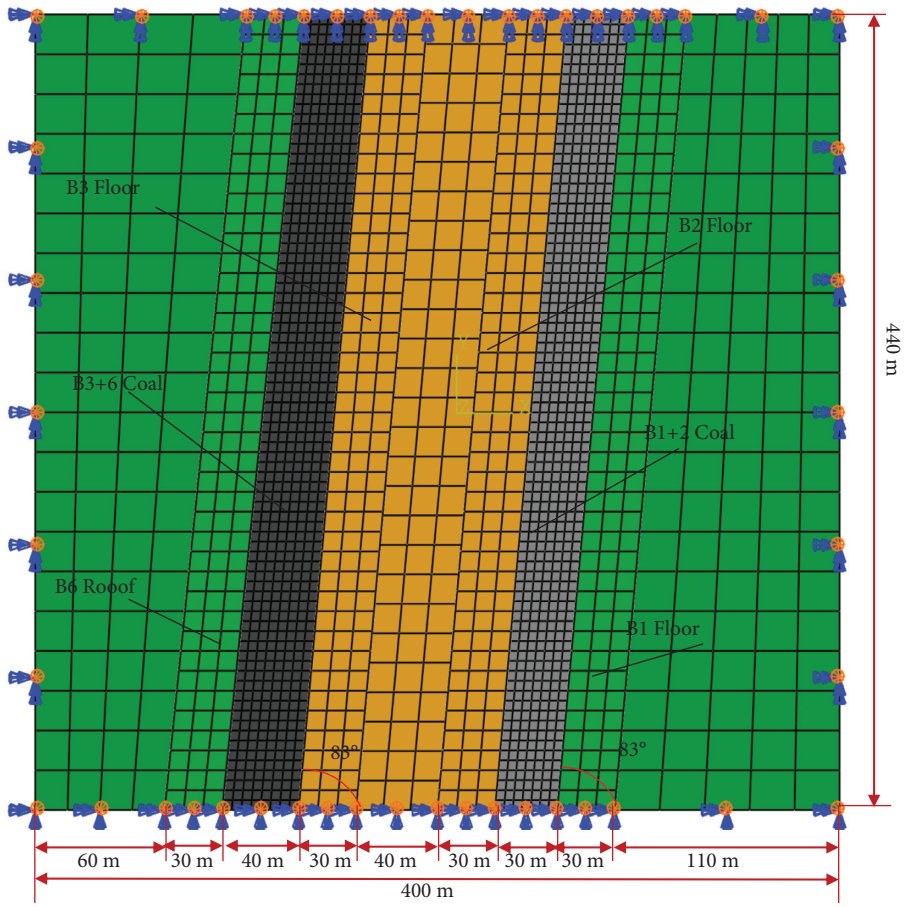

Figure 4: Numerical model diagram.

Table 3: The parameters of numerical simulation.

Coal & rock	Density (kg/m^3)	Tensible strength (MPa)	Cohesion (MPa)	Elastic modulus (GPa)	Shear modulus (GPa)	Friction angle (°)	Poisson ratio
B6 roof	2478	5.70	7.00	2.64	1.03	28.5	0.28
B3+6 coal	1336	1.20	2.40	0.196	0.081	27.0	0.21
Rock pillar	2509	3.99	3.26	1.53	0.603	30.2	0.27
B1+2 coal	1318	1.32	2.40	0.183	0.075	31.5	0.22
B1 floor	2478	5.70	7.00	2.64	1.03	28.6	0.28
Yellow sand	1790	0	0.01	0.002	0.001	10.5	0.21

The rock pillar on the right side of the B3 laneway does not generate damage.

From +525 m level to 450 m level, the destruction of the rock pillar only occurs on the B2 roof, the overall structure is stable. This indicates that there are no damage to the left bottom of the middle rock pillar by the rotation of the crowbar. Under the large horizontal structural stress, the stress concentration of the suspended roof caused the rock burst in the Wudong coal mine, which is consistent with the previous results.

5.3. Analysis of Stress Law of Different Levels. In the mining process, the B1+2 and B3+6 coal mining faces are not allowed to work simultaneously, so a reasonable sequence should be studied. According to the data recorded by the intelligent digital strain gauge, the curves of stress values were at +525 m level, +500 m level, +475 m level, and +450 m level. The pressure cells located in B3+6 and B1+2 coal seams are damaged when advancing arrives at every levels, so the values will be missed in curves, as shown in Figure 7.

The geostatic stress before mining was obtained. The stress of the surrounding rock was released, and the values decreased after mining at different levels. The energy of the surrounding rock of the B3+6 coal seam was released, and the stress value was less than the geostatic stress slightly. The path of the horizontal stress was cut off, then the pressure of the B1+2 coal seam and the surrounding rock was unloaded, and the stress value was reduced greatly.

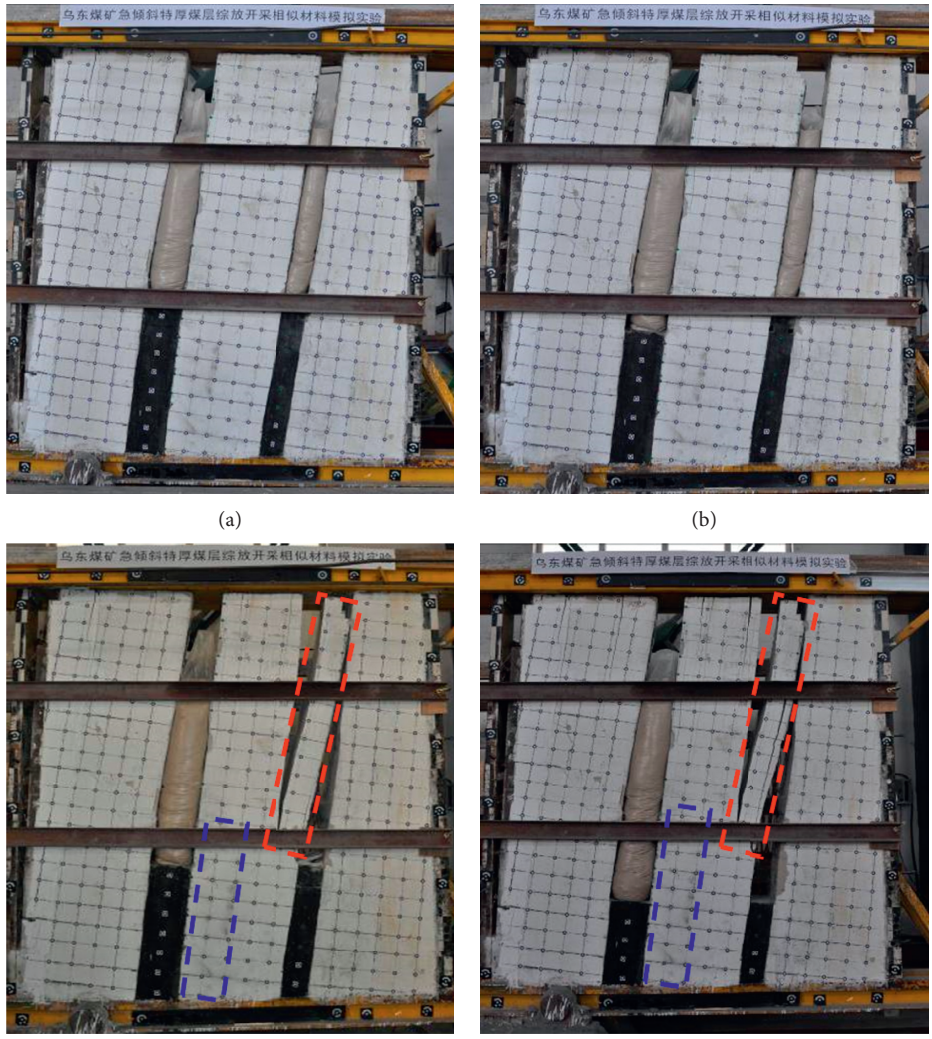

Figure 5: The characteristic of fracture at different levels. (a) +525 m level. (b) +500 m level. (c) The filling body was removed. (d) +450 m level.

With the continuous advancement of the coal mining face, the difference between the geostatic stress and the stress value from 0.3 MPa increased to 0.6 MPa.

The mining of B1+2 coal seams reduced its surrounding rock stress accordingly and had the decompression effect on the B3+6 coal seam. Although B1+2 coal seams have been mined, the horizontal stress of the B3+6 coal seam is still transmitted to the surrounding rocks with a maximum difference of 0.2 MPa.

In general, mining B3+6 coal seams in the Wudong coal mine first produced a substantial decompression to B1+2 coal seams and the surrounding rock. For the similar steeply inclined coal seams, the opposite side should be mined first, which can release the energy in the rock in advance, thus preventing the rock burst effectively when multiple working faces are working.

5.4. Analysis of the Result of Numerical Simulation. During the excavation from the surface to +590 m levels in the simulation, the gob was not filled with the yellow soil. Then, the filling body was filled into the gob to +500 m level. In order to reduce the stress concentration caused by the curb, the filling body was filled from the surface to the mining face.

As shown in Figure 8(a), when excavation reaches +590 m level without the filling body, the stress concentration zones are distributed mainly at the B6 roof, middle rock pillar, and B1 floor with a maximum stress value of 8.20 MPa. The middle rock pillar is prone to rock burst, indicating that the damage of the rock pillar is the main reason for the rock burst, in the steeply inclined coal seam.

As shown in Figure 8(b), the stress concentration zones disappear effectively at +522 m level, with the filling body, and the maximum stress values of the movement of the B6 roof and the B3 floor reduce from 8.2 MPa to 6.3 MPa. While stress concentration range of the B1 floor extends to the surrounding rock because of the pressure of the filling body. A small stress concentration zone is located at the top of the B2 roof, indicating that the stress of the middle rock pillar tends to increase, and this area is dangerous.

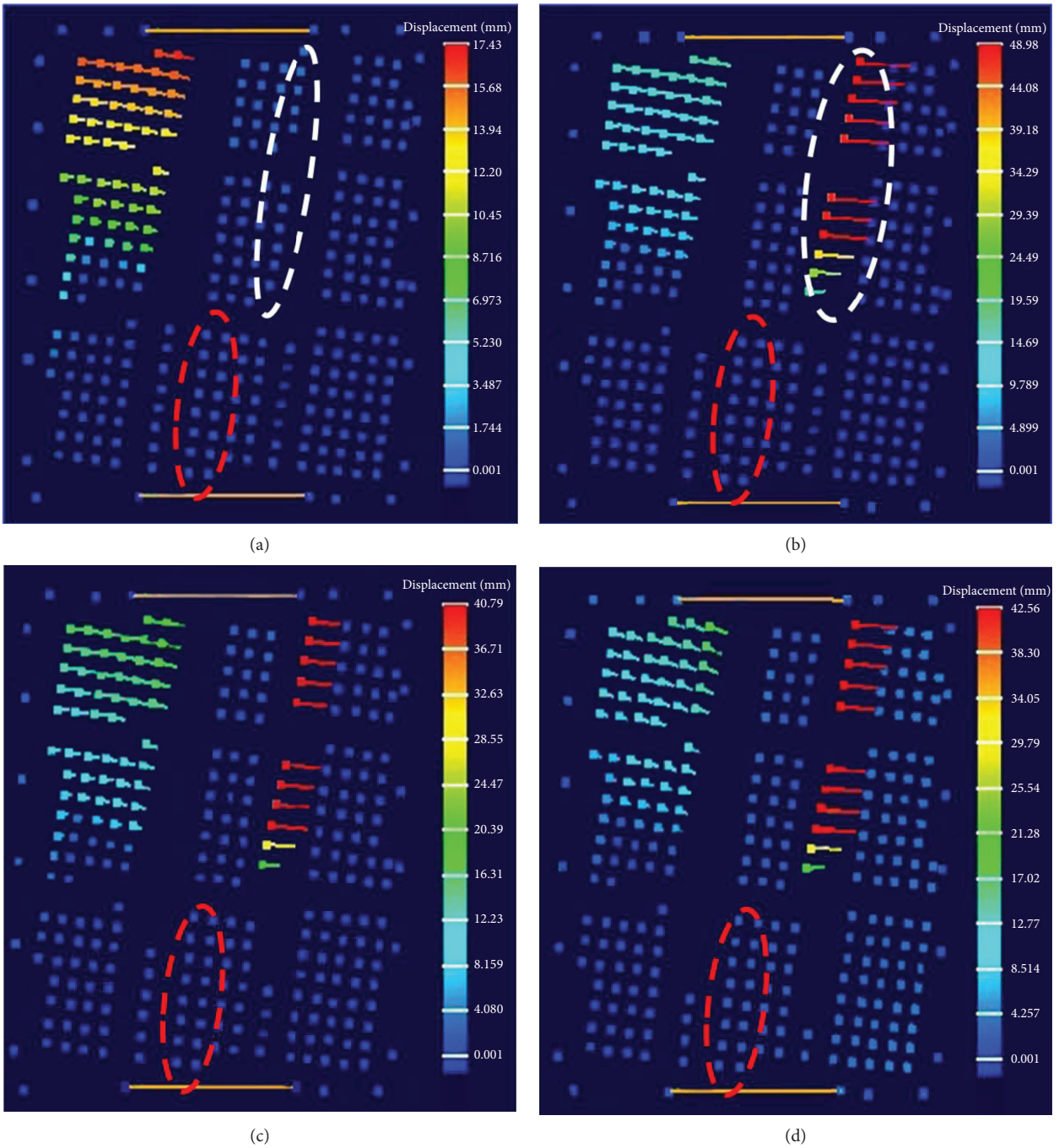

Figure 6: The vectograph of overburden strata. (a) +525 m level. (b) +500 m level. (c) +475 m level. (d) +450 m level.

When the excavation reaches +500 m level, the filling body in the B1+2 goaf is removed; then, the stress concentration zone of the B2 roof appears again, as shown in Figure 8(c). For the B3+6 goaf, the filling body still exists. The stress change is not obvious compared with the +522 m level. Due to the right side of the rock pillar losing the support from the filling body, the stress value increases sharply under the effect of gravity and horizontal stress. Meanwhile, the stress value of the B1 floor is reduced, as shown in Figure 8(b).

For the filling body, the stress value increased gradually with the advance of mining. When mining faces are at +522 m level, the stress value of the filling body is only 0.58 MPa. However, the stress value of the filling body at +500 m level is 3.12 MPa, which is five times the stress value at +500 m level, indicating that the filling body can absorb the energy generated by the deformation of the surrounding rock. The high-stress concentration zone of the surrounding rock disappears accordingly.

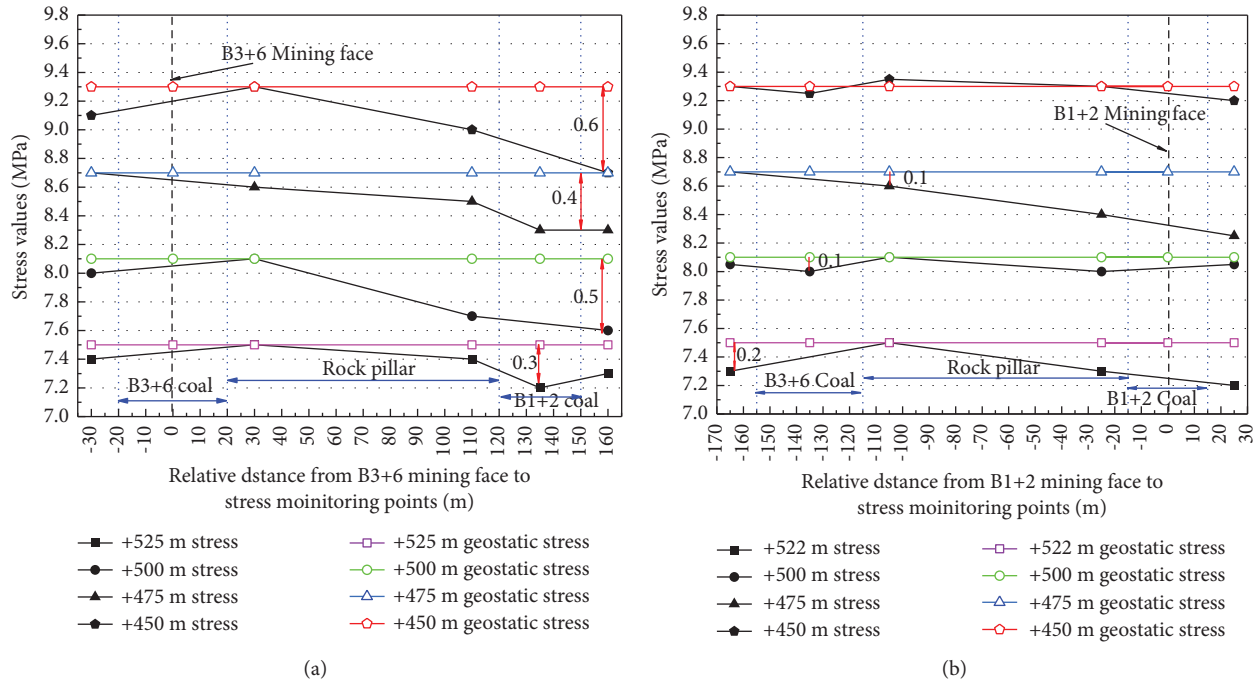

Figure 7: The stress distribution of overburden strata at different levels. (a) The stress distribution of the B3+6 coal seam after mining. (b) The stress distribution of the B1+2 coal seam after mining.

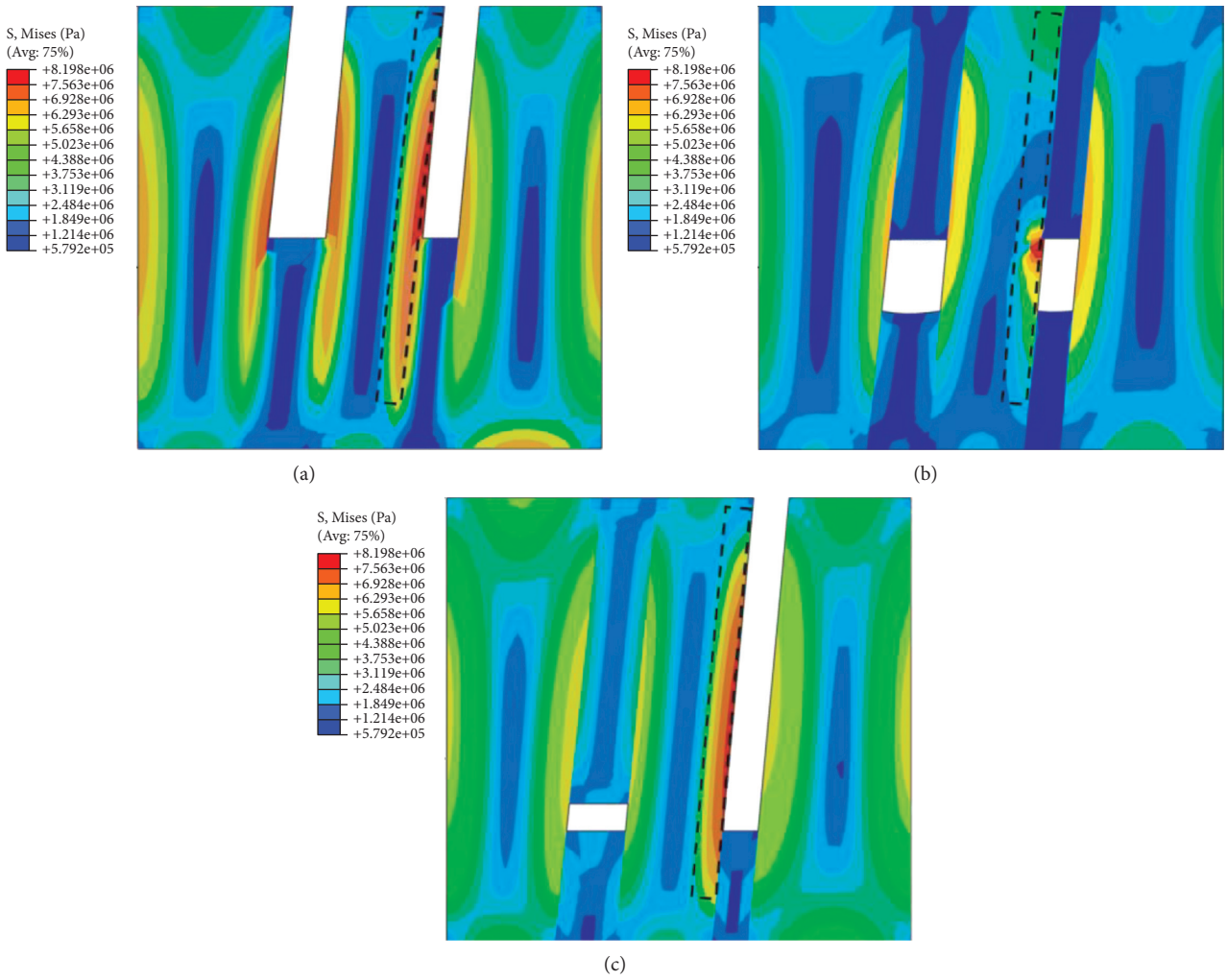

Figure 8: The stress distribution of the rock. (a) +590 m level. (b) +525 m level. (c) +500 m level.

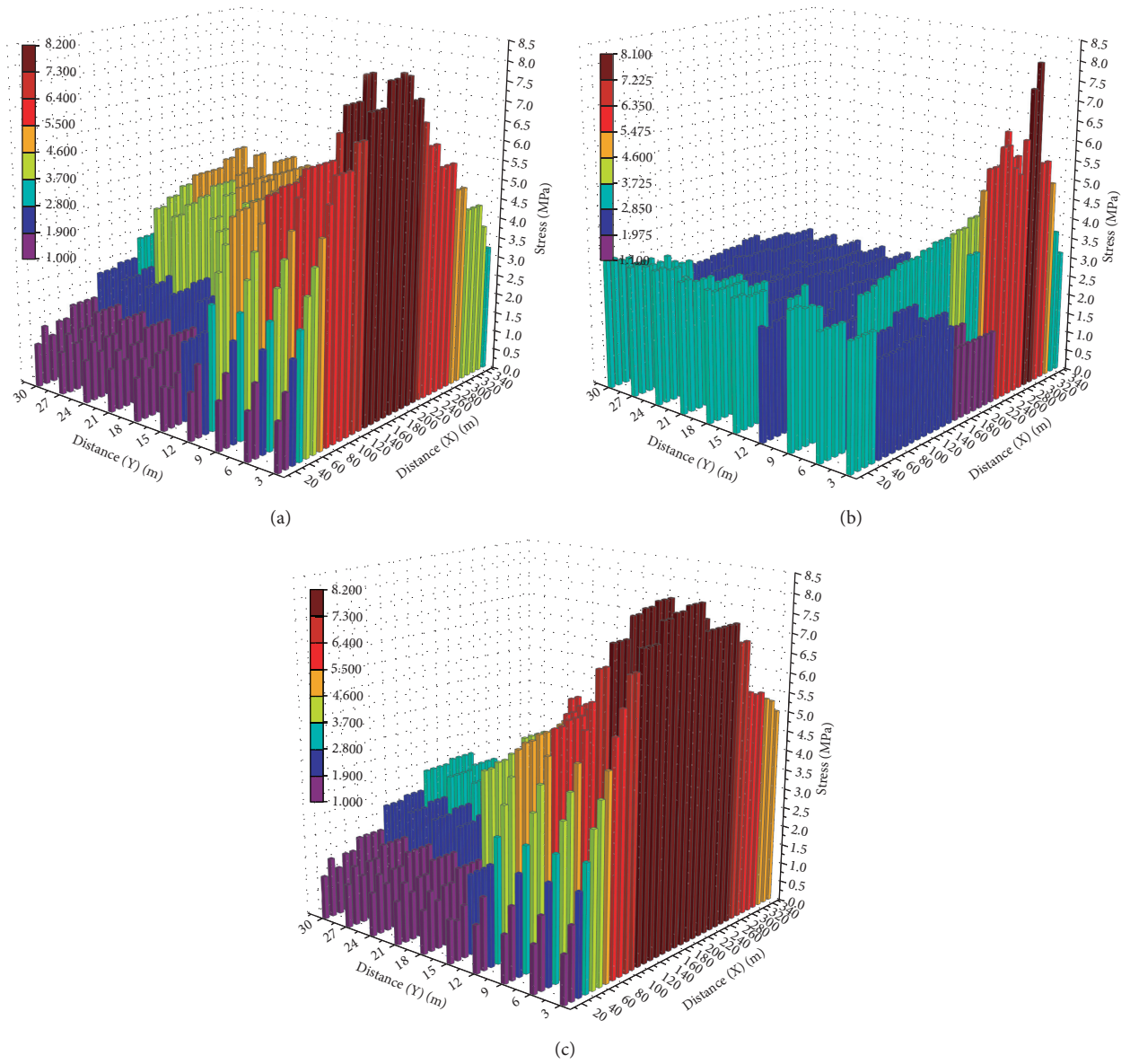

Figure 9: The 3D bars of the stress distribution. (a) +590 m level. (b) +525 m level. (c) +500 m level.

The stress distribution of the B2 roof can be represented by 3D bars (Figure 9). The stress concentration zone reduces by 70% in the B2 roof with the filling body. However, when the filling body is removed, the stress concentration zone appears again and extends to 300 m from 240 m. In addition, there is an isolated high-stress point at a 250 m distance. The results are consistent with the results of the physical similarity simulation experiment described in the last chapter.

The filling body can significantly reduce stress concentration hazards and share the horizontal stress and ground stress in steeply inclined coal seams. For the steeply inclined coal seam, the stability of the middle rock pillar is very important to protect against the rock burst, and the filling body can effectively provide support for the rock pillar on the tilt side, to prevent rock burst.

6. Conclusions

(1) The main factor causing a rock burst disaster in a steeply inclined coal seam is the abnormal stress distribution in the middle rock pillar rather than the stress-lever-effect of the deeper rock pillar.

(2) The filling body can eliminate the stress concentration zone largely and prevent the rock burst. The cut-and-fill mining technology is as effectual to steeply inclined coal seams as to flat coal seam.

(3) Reasonable mining sequence is important for preventing rock burst in a steeply-inclined coal seam. The opposite side of the coal seam should be mined first to release the energy in the rock in advance.

Data Availability

The data used to support the findings of this study are available from the corresponding author upon request.

Conflicts of Interest

The authors declare no conflicts of interest regarding the publication of this study.

Acknowledgments

This research was funded by the Special Funds for the Construction of First-Class Disciplines (552001002048).

References

[1] H. Lan, "Prevention measures and types of mine strata pressure bump occurred in shallow depth seam," *Coal Science and Technology*, vol. 42, no. 1, pp. 9–13, 2014.

[2] Y. S. Pan, Z. H. Li, and M. T. Zhang, "Distribution, type, mechanism and prevention of rockburst in China," *Chinese Journal of Rock Mechanics and Engineering*, vol. 22, no. 11, pp. 1844–2185, 2003.

[3] Z. Mróz and P. Nawrocki, "Deformation and stability of an elasto-plastic softening pillar," *Rock Mechanics and Rock Engineering*, vol. 22, no. 5, pp. 69–108, 1989.

[4] Y. C. Yin, J. C. Zou, Y. B. Zhang, and Y. Qiu, "Experimental study of the movement of backfilling gangues for goaf in steeply inclined coal seams," *Arabian Journal of Geosciences*, vol. 11, no. 12, pp. 1–8, 2018.

[5] F. X. Jiang, J. L. Wem, W. S. Bai, G. L. Wang, and M. Li, "Rock burst risk in surrounding abscission layer overlying high key strata in deep strip mining mines," *Journal of China University of Mining & Technology*, vol. 47, no. 1, pp. 40–47, 2018.

[6] Y. Deng and S. Wang, "Feasibility analysis of gob-side entry retaining on a working face in a steep coal seam," *International Journal of Mining Science and Technology*, vol. 24, no. 4, pp. 499–503, 2014.

[7] H. Y. Dai, T. J. Guo, and A. J. Liu, S. H. Yi, G. Y. Wang, B. Kong, and B. Ju, The mechanism of strata and surface move-ments induced by extra-thick steeply inclined coal seam applied horizontal slice mining," *Journal of China Coal Society*, vol. 38, no. 1, pp. 1110–1115, 2013.

[8] X. P. Lai, M. F. Cai, F. H. Ren, P. F. Shan, F. Cui, and J. T. Cao, "Study on dynamic disaster in steeply deep rock mass condition in urumchi coalfield," *Shock and Vibration*, vol. 2015, Article ID 465017, 8 pages, 2015.

[9] B. Zhang and S. Cao, "Study on first caving fracture mechanism of overlying roof rock in steep thick coal seam," *International Journal of Mining Science and Technology*, vol. 25, no. 1, pp. 133–138, 2015.

[10] W. J. Ju, J. W. Zheng, and D. Wei, "Study on the causes and control technology about the coal bump in multi-layered mining roadwy in steep-think coal seams," *Journal of Mining & Safety Engineering*, vol. 36, no. 2, pp. 280–289, 2019.

[11] M. Jawed and R. K. Sinha, "Design of rhombus coal pillars and support for Roadway Stability and mechanizing loading of face coal using SDLs in a steeply inclined thin coal seam-a technical feasibility study," *Arabian Journal of Geosciences*, vol. 415, pp. 1–14, 2018.

[12] S. Zhang, L. Lu, Z. Wang, and S. Wang, "A physical model study of surrounding rock failure near a fault under the influence of footwall coal mining," *International Journal of Coal Science & Technology*, vol. 8, no. 4, pp. 626–640, 2021.

[13] X. P. Lai, J. J. Dai, and C. Liu, "Analysis on hazard characteristics of overburden structure in steeply inclined coal seam," *Journal of China Coal Society*, vol. 45, no. 1, pp. 122–130, 2020.

[14] J. Wang, D. B. Apel, Y. Pu, R. Hall, C. Wei, and M. Sepehri, "Numerical modeling for rockbursts: a state-of-the-art review," *Journal of Rock Mechanics and Geotechnical Engineering*, vol. 13, no. 2, pp. 457–478, 2021.

[15] J. Wang, D. B. Apel, A. Dyczko et al., "Investigation of the rockburst mechanism of driving roadways in close-distance coal seam mining using numerical modeling method," *Mining, Metallurgy & Exploration*, vol. 38, no. 5, pp. 1899–1921, 2021.

[16] P. Malkowski, Z. Niedbalski, and T. Balarabe, "A statistical analysis of geomechanical data and its effect on rock mass numerical modeling: a case study," *International Journal of Mining Science and Technology*, vol. 8, no. 2, pp. 312–323, 2021.

[17] Q. Zhang, J. X. Zhang, J. Q. Wang, and P. Huang, "Theoretical research and its engineering practice on critical backfill ratio in backfill mining," *Journal of China Coal Society*, vol. 42, no. 12, pp. 3081–3088, 2017.

[18] Y. Chen, F. X. Jiang, and D. C. Meng, "Prevention mechanism of rock burst in backfill mining in extra-thick coal seam with deep shaft," *Journal of Mining & Safety Engineering*, vol. 37, no. 5, pp. 970–975, 2020.

[19] Q. Zhang, J. X. Zhang, F. Ju, and M. Li, "Back-fill body's compression ratio design and control theory research in solid backfill coal mining," *Journal of China Coal Society*, vol. 39, no. 1, pp. 64–71, 2014.

[20] Y. Q. Hu, Y. S. Zhao, and D. Yang, "Study of 3D simulation on breakage for coal floor in mining above aquifer," *Chinese Journal of Rock Mechanics and Engineering*, vol. 22, no. 8, pp. 1239–1243, 2003.

[21] H. C. Li, *Similar Simulation Test of Mine Presure*, China University of Mining and Techonlogy Press, Xuzhou, China, 1987.

[22] Q. Ye, G. Wang, Z. Jia, C. Zheng, and W. Wang, "Similarity simulation of mining-crack-evolution characteristics of overburden strata in deep coal mining with large dip," *Journal of Petroleum Science and Engineering*, vol. 165, pp. 477–487, 2018.

[23] D. H. Li, X. Q. He, and J. Q. Chen, "Inducing mechanism of rock burst occoring in steeply-inclined coal seam of Wudong coal mine," *Journal of China University of Mining & Technology*, vol. 49, no. 5, pp. 838–840, 2020.

[24] R. K. Sinha, M. Jawed, and S. Sengupta, "Influence of rock mass rating and in situ stress on stability of roof rock in bord and pillar development panels," *International Journal of Mining and Mineral Engineering*, vol. 6, no. 3, pp. 258–275, 2015.

[25] T. T. Du, K. Li, H. Lan, and X. Liu, "Rockburst process analysis in steeply-inclined extremely-thick coal seam," *Journal of Mining & Safety Engineering*, vol. 35, no. 1, pp. 141–145, 2018.